

Electronic Supplementary Information (ESI)

Site-Specific Catalysis on Micro-Catalytic Chip by Synergistic Silencing of Site-Directing Electronic Effects of Functional Groups in Aromatics

*Rakesh Sen¹, Kousik Das¹, Subhrokoli Ghosh², Anand Dev Ranjan², Khokan Manna¹, Ayan
Banerjee^{2*} and Soumyajit Roy^{1*}.*

¹EFAML, Materials Science Centre, Department of Chemical Sciences, Indian Institute of
Science Education and Research Kolkata, Mohanpur 741246, India

²Light Matter Lab, Department of Physical Sciences, Indian Institute of Science Education
and Research Kolkata, Mohanpur 741246, India

Email: s.roy@iiserkol.ac.in (SR); ayan@iiserkol.ac.in (AB)

Table of contents

1. Experimental Section	3
1.1. General method and materials	3
1.2. Synthesis of TBA ₆ [PV ₃ W ₉ O ₄₀]:	4
1.3. Synthesis of PPy/MWCNT composite	4
1.4. Synthesis of POM/PPy/MWCNT composite	4
1.5. Description of optical tweezers set up and fabrication of trails	5
Figure S1. Schematic cartoon of optical tweezer setup used to fabricate micro-catalytic patterns	6
Figure S2: EDX of patterned composite material showing uniform abundance of P, V and W atoms on the surface of composite material which also confirms the uniform distribution of POM clusters.	7
Figure S3: X-ray photoelectron spectroscopy (XPS) analysis of trail material obtained by scrapping them off from the micro-catalytic chip surface. Before reaction: (a) XPS survey spectrum demonstrating the presence of C, N, O, P, V, W and O in the sample. (b) High resolution N 1s XPS scan, (c) High resolution P 2p XPS scan. After reaction: (c) XPS survey spectrum demonstrating the presence of C, N, O, P, V, W and O in the sample. (d) High resolution N 1s XPS scan, (e) High resolution P 2p XPS scan	8
Figure S4: IR spectra of p-nitroaniline taken in pure form and after drop casting on the micro-catalytic trails. The inset zoomed in IR regions show red shifts in N-H stretching (both symmetric and asymmetric) and N-H bending vibrations of -NH ₂ group and N=O Stretching (both symmetric and asymmetric) frequencies of -NO ₂ group. This indicates towards possible H-bonding of these moieties with the oxo-terminals of the trail surface.	9
Figure S5: High Resolution O1s X-Ray Photoelectron Spectra (XPS) of deposited trail materials captured before and after the reaction. The increase in oxygen vacancy relative to lattice oxygen population in the spectra captured after the reaction supports our proposed tentative reaction pathway where the oxidation of a docked substrate molecule (aromatic amines) is facilitated via an oxo transfer from the oxo-surface of the catalytic trail generating an oxygen vacancy in the surface.	10
Figure S6: GC-MS characterization of the products at different reaction conditions as mentioned in Table 1. The Mass spectra of the products and reactant eluted at different times are shown in the inset figures	11
Table S1. Product Distribution with variation of Polyoxometalate component	12
Table S2. Nitro Selectivity Distribution with variation of Solvent	13
Table S3. Effect of MWCNT:PPy:POM ratio on product distribution	14
References	15

1. EXPERIMENTAL SECTION

1.1. General method and materials:

All the chemicals were purchased from either Merck or Sigma-Aldrich and were used as obtained. MWCNT was purchased from Techinstro. The synthesis and purification of $\text{Na}_9[\text{A-}\alpha\text{-PW}_9\text{O}_{34}]$ and $\text{TBA}_5\text{H}_4[\text{P}_2\text{V}_3\text{W}_{15}\text{O}_{62}]$ were done according to literature procedures.^{1, 2} Bruker ALPHA FTIR spectrometer fitted with ATR module was used to record the ATR-IR spectra in the range of 500–4000 cm^{-1} . The TGA was performed using a Mettler Toledo TGA/SDTA 851e system at a heating rate of 10°C min^{-1} in N_2 atmosphere. A LABRAM HR800 Raman spectrometer was employed using the 633 nm line of a He–Ne ion laser as the excitation source to record Raman Spectra of the sample. The transmission electron micrographs of the composite were primarily taken using a Tecnai 20 transmission electron microscope (FEI Company) operated at an accelerating voltage of 200 kV. The TEM micrographs were processed using SIS software (Soft Imaging System). X-ray photoelectron spectroscopy was performed in a Thermo Fisher Scientific Instruments (K alpha+) instrument using a Al $\text{K}\alpha$ (Monochromatic) source operating with 6 ma beam current and 12 kV energy., where the instrument calibration was performed using the reference binding energy of C 1s at 284.8 eV. Product characterisation and analysis was done using Trace 1300 GC and ISQ qd single quadrupole mass spectrometer with a TG-5MS capillary column (30 m \times 0.32 mm \times 0.25 μm) supplied by Thermo Fisher Scientific, India. The conversion of aniline in the reaction and the product selectivity have been determined using the following equations already reported in the literature.³

$$\text{Conversion (mol\%)} = \frac{\text{Initial mol\% of aniline} - \text{Final mol\% of aniline}}{\text{Initial mol\% of aniline}} \times 100$$

$$\text{Selectivity of a Product (\%)} = \frac{\text{GC peak area of the concerned product}}{\text{Sum of the GC peak areas of all the products}} \times 100$$

1.2. Synthesis of TBA₆[PV₃W₉O₄₀]:

The procedure to synthesise the POM was similar to that described in the literature.¹ NaVO₃ (0.3 g, 2.5 mmol) was added to 10 mL of 1.0 M sodium acetate/acetic acid buffer (pH 4.8). Now, 2 g (0.75 mmol) of Na₈H[PW₉O₃₄] was added to this solution and stirred for 48 h at 25°C. Now to this, 1.5 g of solid KCl was added and stirred for 30 min followed by the addition of Methanol (25 mL) to produce tan-orange coloured precipitate which was filtered to give 2.2 g of powder.

Now, 0.55 g of this K-salt was dissolved in minimum amount of distilled water and to it 0.65 g of TBAB was added and the solution was stirred for 12 h. This gives rise to golden orange coloured precipitate which was then filtered and washed with minimum amount of water.

1.3. Synthesis of PPy/MWCNT composite:

The composite was synthesised by *in-situ* chemical oxidative polymerization of pyrrole with FeCl₃ in presence of MWCNT. At first, the solution of oxidising agent was prepared by dissolving 193 mg of FeCl₃.6H₂O in minimum amount of distilled water (1:2.4 Monomer: Oxidant). Then it was added slowly into a solution of 20 mg pyrrole and 10 mg MWCNT in 20 ml of distilled water with a constant sonication at a temperature of about -3 °C, followed by further sonication in ice bath for 4 hrs. The composite thus obtained was filtered and rinsed several times with distilled water. Then it was dried under vacuum at room temperature for 48 h.

1.4. Synthesis of POM/PPy/MWCNT composite

The as-synthesized PPy/MWCNT composite material (10 mg) was added to a solution of TBA₆[PV₃W₉O₄₀] (30 mg) in deionized water (10 mL). The mixture was ultra-sonicated for 3

h, and then stirred for another 5 h at room temperature. This mixture was used directly for catalytic trail formation.

1.5. Description of optical tweezers set up and fabrication of trails

The experimental setup consists of an optical tweezers with a motorized translational stage as shown in the schematic (Fig. S1). A 10 μ l of POM/PPy/MWCNT mixture is taken on a glass coverslip placed on the sample stage of the inverted microscope. This inverted microscope (Zeiss Axiovert A1 Observer) consists of a high numerical aperture objective (1.4NA) with a translating sample stage which is also called optical tweezers. When a highly focused gaussian beam (1064 nm) after passing through the 100x objective falls on the sample material kept on the sample stage then it creates a local hot spot which results in formation of micro-bubbles. Now, as we move the translation stage of the optical tweezers microscope, the focal point of the laser gets shifted – concomitantly translating the bubble, leading to self-assembly, and eventual patterning of the composite material in the wake of the bubble. The length and width of the patterns can be controlled by sample stage speed and power of laser at the focal plane of the stage. The speed of the sample stage is controlled using a joystick (Ludl MAC5000 XY) connected to the translational stage which has a travel range of 130 \times 100 mm with resolution of 100 nm. Laser controller provides the intensity control at the focal plane of the objective. Although we can generate laser spots of power more than 100mW but we confine ourself to a power less than 60 mW for the experiment in order to minimize any deterioration of the dispersed sample due the laser. Thus, by moving the translation stage in a pre-designed manner and controlling the laser power, we obtained a continuous pattern of our composite material in the micro-catalytic chip.

Figure S1

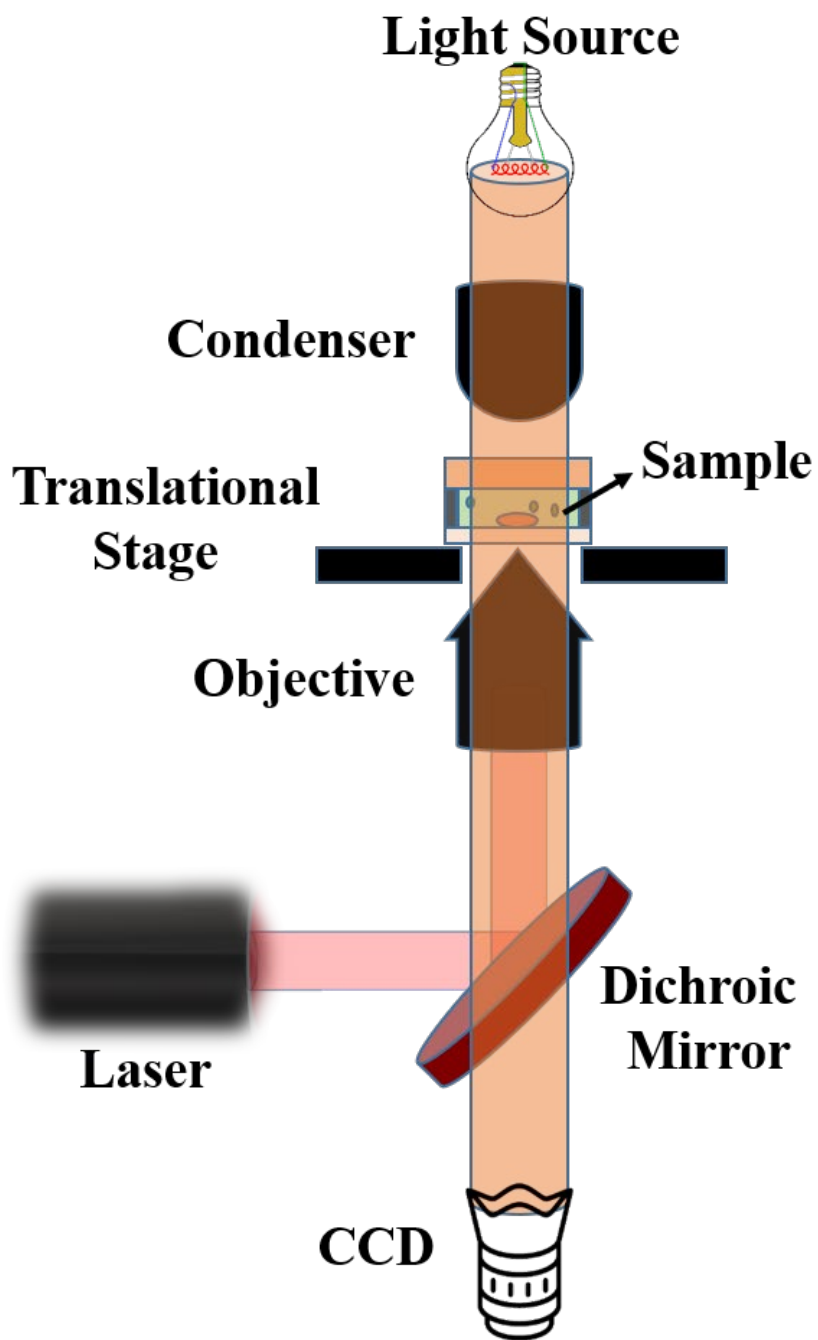


Figure S1. Schematic cartoon of optical tweezer setup used to fabricate micro-catalytic patterns

Figure S2

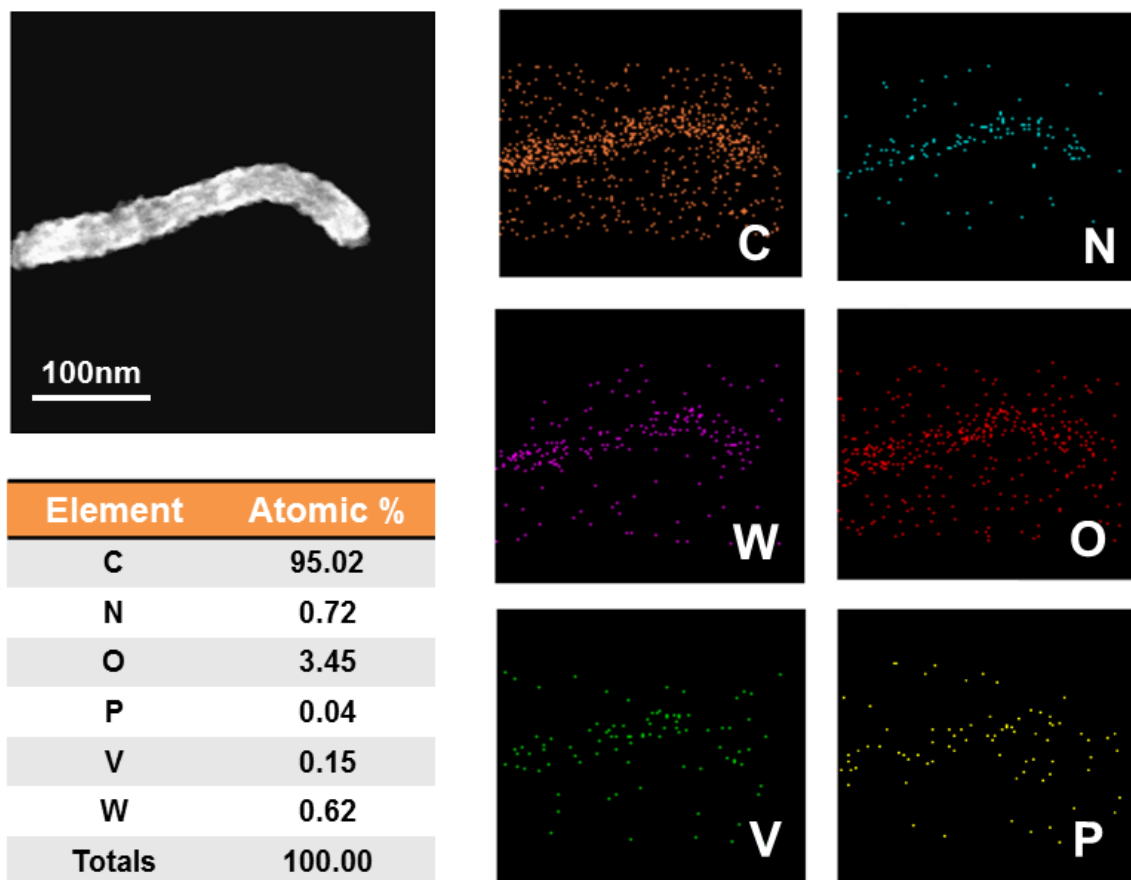


Figure S2: EDX of patterned composite material showing uniform abundance of P, V and W atoms on the surface of composite material which also confirms the uniform distribution of POM clusters.

Figure S3

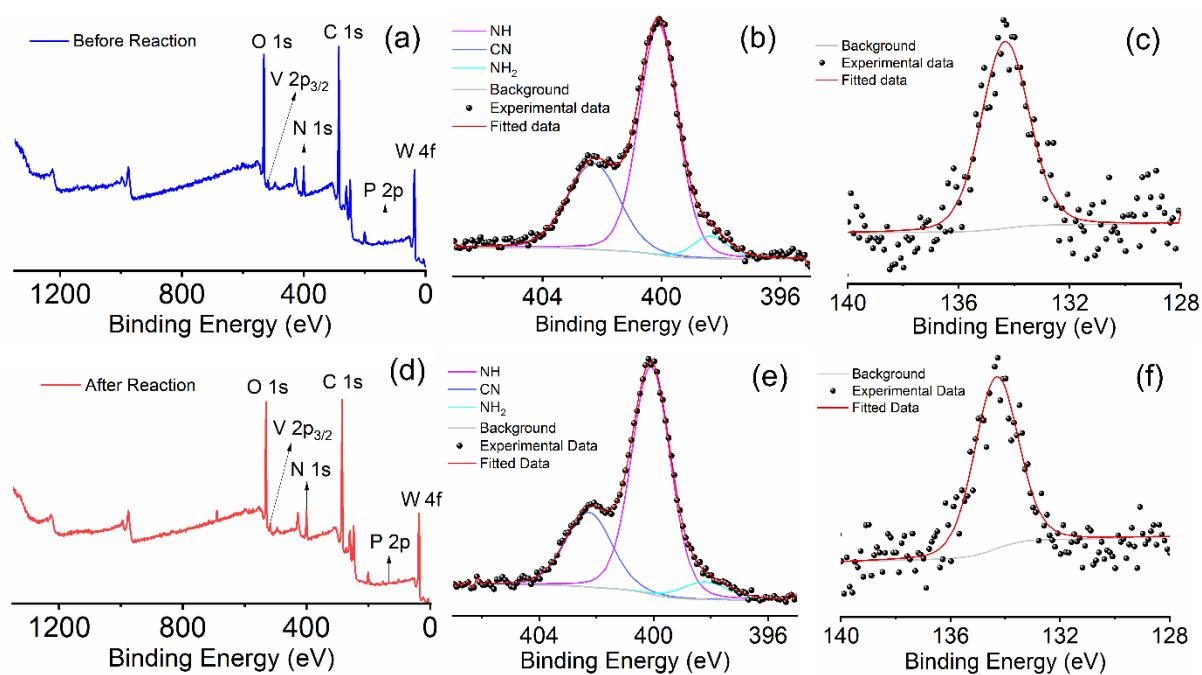


Figure S3: X-ray photoelectron spectroscopy (XPS) analysis of trail material obtained by scrapping them off from the micro-catalytic chip surface. Before reaction: (a) XPS survey spectrum demonstrating the presence of C, N, O, P, V, W and O in the sample. (b) High resolution N 1s XPS scan, (c) High resolution P 2p XPS scan. After reaction: (d) XPS survey spectrum demonstrating the presence of C, N, O, P, V, W and O in the sample. (e) High resolution N 1s XPS scan, (f) High resolution P 2p XPS scan

Figure S4

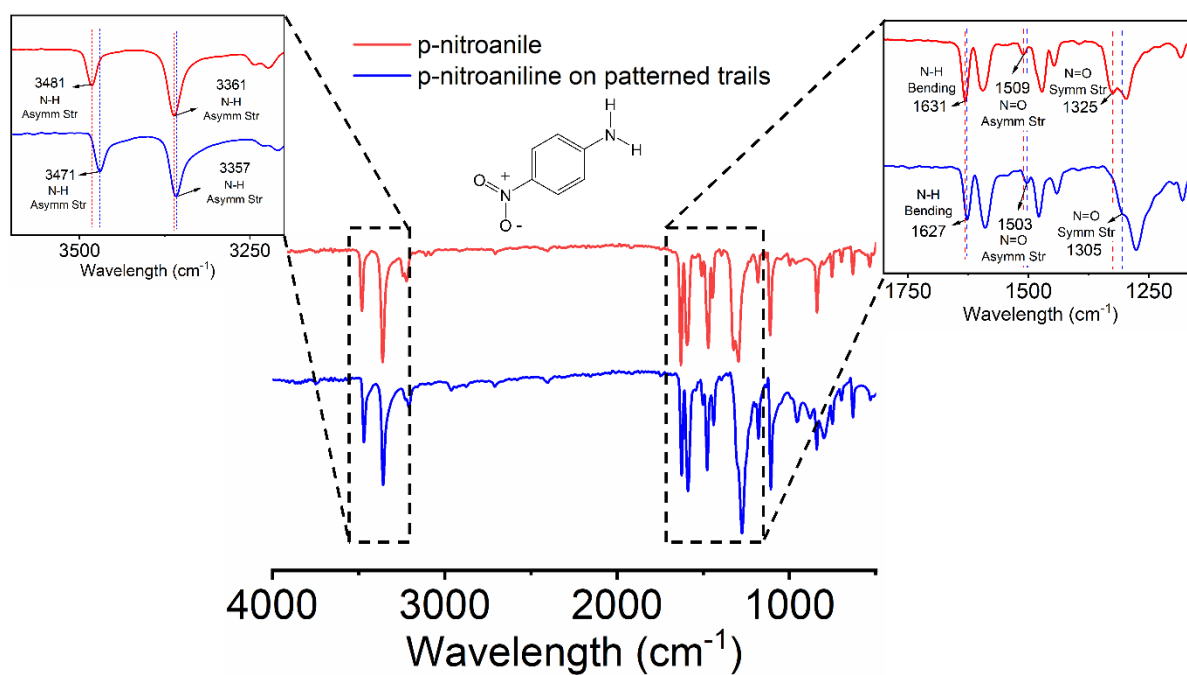


Figure S4: IR spectra of p-nitroaniline taken in pure form and after drop casting on the micro-catalytic trails ^{4,6}. The inset zoomed in IR regions show red shifts in N-H stretching (both symmetric and asymmetric) and N-H bending vibrations of -NH₂ group and N=O Stretching (both symmetric and asymmetric) frequencies of -NO₂ group. This indicates towards possible H-bonding of these moieties with the oxo-terminals of the trail surface.

Figure S5

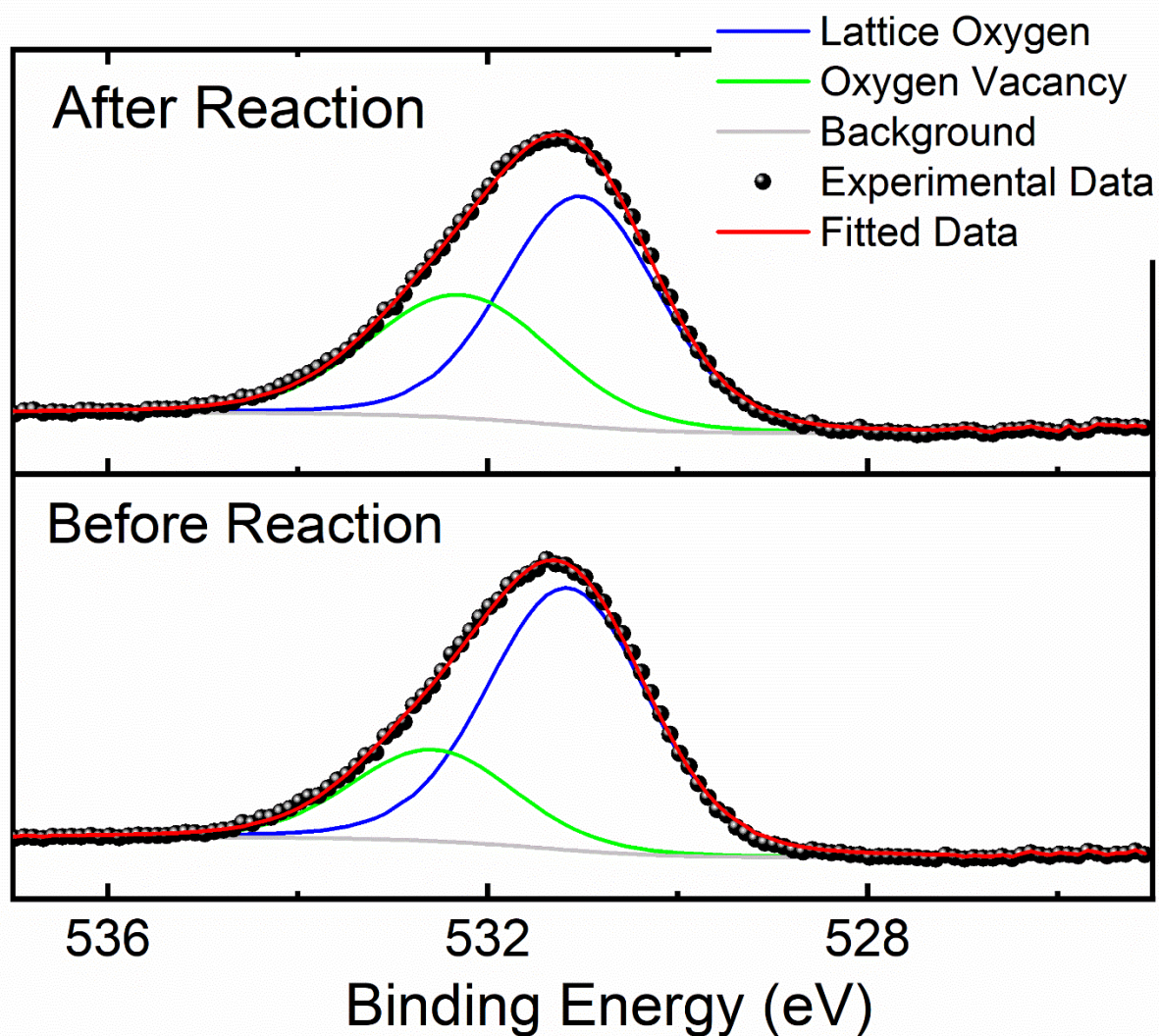


Figure S5: High Resolution O1s X-Ray Photoelectron Spectra (XPS) of deposited trail materials captured before and after the reaction. The increase in oxygen vacancy relative to lattice oxygen population in the spectra captured after the reaction supports our proposed tentative reaction pathway where the oxidation of a docked substrate molecule (aromatic amines) is facilitated via an oxo transfer from the oxo-surface of the catalytic trail generating an oxygen vacancy in the surface.

Figure S5

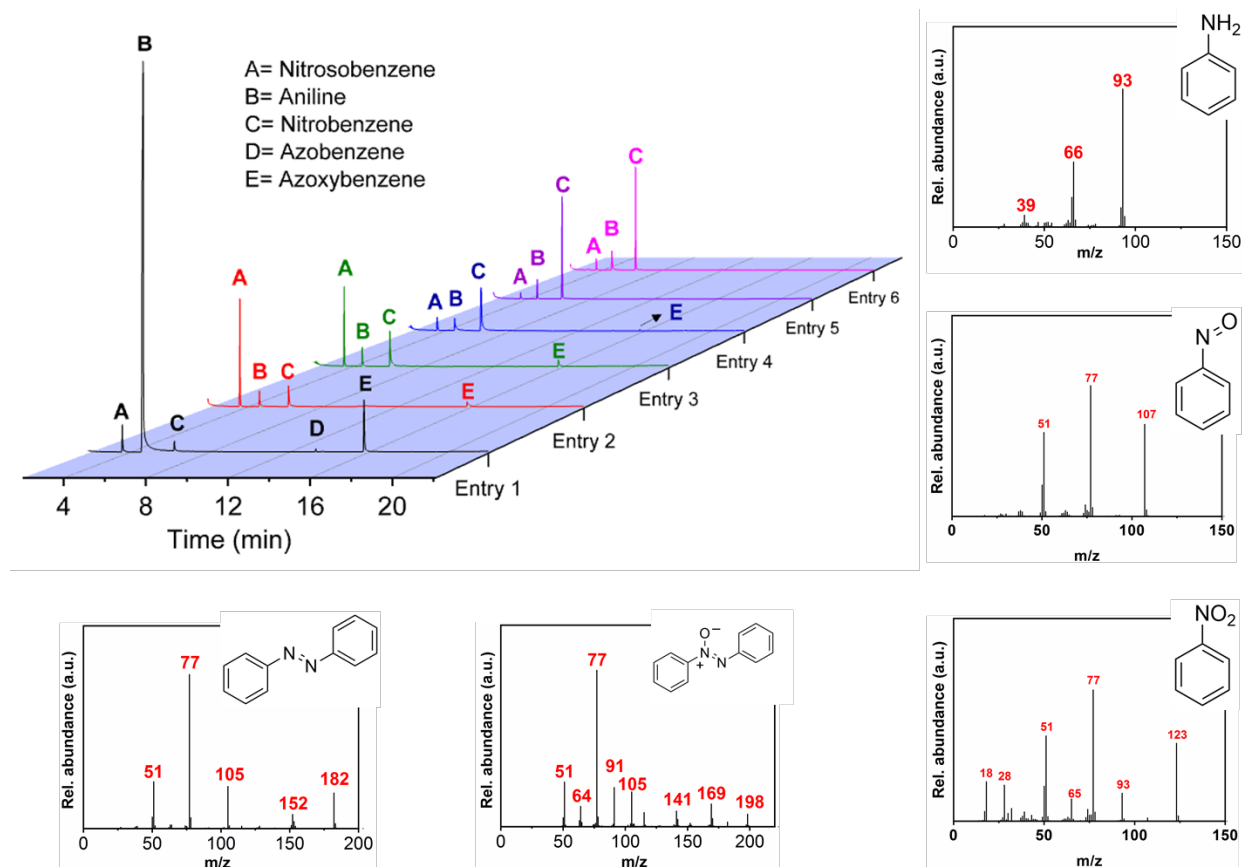


Figure S6: GC-MS characterization of the products at different reaction conditions as mentioned in Table 1. The Mass spectra of the products and reactant eluted at different times are shown in the inset figures

Table S1

Entry	Polyoxometalate Component	Conversion (%)	Products Selectivity (%)			
			Nitro	Nitroso	Azoxy	Azo
1	H ₃ PW ₁₂ O ₄₀	45	87	13	--	--
2	K ₆ PV ₃ W ₉ O ₄₀	74	41	55	4	--
3	[bmim] ₆ PV ₃ W ₉ O ₄₀	81	63	37	--	--
4	TBA ₆ PV ₃ W ₉ O ₄₀	83	95	5	--	--
5	TBA ₅ H ₄ [P ₂ V ₃ W ₁₅ O ₆₂]	80	85	15	--	--

Table S1. Product Distribution with variation of Polyoxometalate component

Table S2

Entry	Solvent	Conversion (%)	Nitro Selectivity (%)
1	DCM	36	39
2	MeCN	83	85
3	DMSO	40	46
4	H ₂ O	22	55
5	H ₂ O:MeCN (1:1)	45	60

Table S2. Nitro Selectivity Distribution with variation of Solvent

Table S3

Entry	MWCNT:PPy:POM (By weight)*	% Convsn	% PhNO₂	% PhNO	Comment
1	1:2:9	83	95	5	--
2	1:1:9	--	--	--	Discontinuous trail formation
3	1:2:5	62	63	37	--
4	1:2:12	84	91	9	Trail formation is very difficult
5	1:2:2	28	41	59	--
6	3:2:9	72	92	8	--

* Weight ratio of individual components taken in preparation of pre-catalyst precursor cocktail

Table S3. Effect of MWCNT:PPy:POM ratio on product distribution

References

1. P. J. Domaille, *Journal of the American Chemical Society*, 1984, **106**, 7677-7687.
2. R. G. Finke, B. Rapko, R. J. Saxton and P. J. Domaille, *Journal of the American Chemical Society*, 1986, **108**, 2947-2960.
3. R. Meenakshi, K. Shakeela, S. Kutti Rani and G. Ranga Rao, *Catalysis Letters*, 2018, **148**, 246-257.
4. M. K. Trivedi, A. Branton, D. Trivedi, G. Nayak, K. Bairwa and S. Jana, *Insights in Analytical Electrochemistry*, 2015, **1**.
5. R. Friedel, *The Journal of Physical Chemistry*, 1958, **62**, 1341-1342.
6. J. A. Lee-Thorp, J. E. Rüede and D. A. Thornton, *Journal of Molecular Structure*, 1978, **50**, 65-71.